Attenuation of LDH-A expression uncovers a link between glycolysis, mitochondrial physiology, and tumor maintenance

Valeria R. Fantin,[1,3,4] Julie St-Pierre,[2,3,5] and Philip Leder[1,*]

[1] Department of Genetics, Harvard Medical School and Howard Hughes Medical Institute, Boston, Massachusetts 02115
[2] Dana-Farber Cancer Institute and Department of Cell Biology, Harvard Medical School, Boston, Massachusetts 02115
[3] These authors contributed equally to this work.
[4] Present address: Merck & Co., Inc., Boston, Massachusetts 02115.
[5] Present address: Institut de Recherche en Immunologie et en Cancérologie (IRIC), Université de Montréal Pavillon Marcelle-Coutu, Montréal, Québec, Canada H3T 1J4.
*Correspondence: leder@genetics.med.harvard.edu

Summary

Alterations in cellular metabolism are among the most consistent hallmarks of cancer. Herein we have investigated the relationship between increased aerobic lactate production and mitochondrial physiology in tumor cells. To diminish the ability of malignant cells to metabolize pyruvate to lactate, lactate dehydrogenase A (LDH-A) levels were knocked down by means of LDH-A short hairpin RNAs. Reduction in LDH-A activity resulted in stimulation of mitochondrial respiration and decrease of mitochondrial membrane potential. It also compromised the ability of these tumor cells to proliferate under hypoxia. The tumorigenicity of the LDH-A-deficient cells was severely diminished, and this phenotype was reversed by complementation with the human ortholog LDH-A protein. These results demonstrate that LDH-A plays a key role in tumor maintenance.

Introduction

A distinctive feature of tumor cells is the alteration of their carbohydrate metabolism. In general, normal cells produce most of the ATP from glucose through oxidative phosphorylation (OXPHOS) (Rolfe and Brown, 1997). On the other hand, many cancer cells produce ATP by conversion of glucose to lactate and exhibit lower OXPHOS activity. The ability of malignant cells to produce large amounts of lactic acid was recognized by Warburg in the early 20s (Warburg, 1930). A high rate of conversion of glucose to lactate is coupled to a high rate of glucose uptake and glucose phosphorylation and occurs even in the presence of normal oxygen pressure (Gatenby and Gillies, 2004; Mathupala et al., 1997). The "glycolytic phenotype" appears to confer emerging malignant cells with a selective advantage, which may help to explain in part why this metabolic strategy is commonly observed across tumors. Accelerated glycolysis ensures ATP levels compatible with the demands of fast proliferating tumor cells in a hypoxic environment. Along with increased glutaminolysis, it provides a constant supply of metabolic intermediates that are essential for macromolecule biosynthesis and necessary for cell growth and division (Mazurek and Eigenbrodt, 2003). In addition, the increased glucose uptake could play a role in protection from apoptosis by rendering tumor cells independent of growth factors (Plas and Thompson, 2002). Because reactive oxygen species are natural by-products of mitochondrial respiration, it has been proposed that glucose to lactate conversion may protect cancer cells from oxidative stress (Brand and Hermfisse, 1997).

The molecular basis for the increased rate of glycolysis in cancer cells remained elusive until the 90s. However, it has become clear in recent years that one of the transcriptional programs turned on by oncogenes including *Ras*, *Src*, and *HER-2/Neu* through the stabilization of HIF-1α protein leads to upregulation of most of the enzymes of the glycolytic pathway, as well as the NADH-dependent enzyme that catalyzes the conversion of pyruvate to lactate, lactate dehydrogenase A (LDH-A), and the glucose transporters GLUT-1 and GLUT-3 (Dang and Semenza, 1999; Semenza et al., 2001). In addition, c-*Myc* has also been shown to regulate LDH-A at the transcriptional level (Shim et al., 1997).

Alterations in mitochondrial physiology, in addition to decreasing OXPHOS capacity, have also been linked to malignant transformation (Capuano et al., 1997; Dorward et al., 1997).

SIGNIFICANCE

The near-universal glycolytic switch of cancer cells has been proposed to be an essential tumor trait and a consequence of the cellular adaptation to hypoxia. Our results are consistent with a functional connection between alterations in glucose metabolism and mitochondrial physiology in cancer. The data also reflect that the dependency of tumor cells on glucose metabolism is a liability for these cells under limited-oxygen conditions. Interfering with LDH-A activity as a means of blocking pyruvate to lactate conversion could be exploited therapeutically. Because individuals with complete deficiency of LDH-A do not show any symptoms under ordinary circumstances, the genetic data suggest that inhibition of LDH-A activity may represent a relatively nontoxic approach to interfere with tumor growth.

Higher mitochondrial membrane potential ($\Delta\psi_m$) has been observed in a variety of carcinomas (Chen, 1988), and in cases of chemically induced and oncogene-induced malignant transformation in a variety of cell types (Liang et al., 1999; Zarbl et al., 1987). In the case of colon cells, the transition to the neoplastic state has been correlated with an increase in this mitochondrial parameter (Heerdt et al., 2003). We have previously described the identification of a small molecule, F16, that is selectively toxic to carcinoma cell lines with higher than normal $\Delta\psi_m$ (Fantin et al., 2002). The fact that glycolysis and mitochondrial respiration are tightly coupled processes led us to propose that the correlative high mitochondrial membrane potential and the susceptibility to the lipophilic cation F16 could be related to the lower OXPHOS activity in transformed cells.

To gain some understanding about the dependency of tumor growth on the glycolytic phenotype and the interplay between glycolysis and mitochondrial metabolism, we decided to evaluate the effect of blocking glucose to lactate conversion. To this end, we stably knocked down LDH-A in *neu*-initiated mammary tumor cells that display high glucose dependency, high LDH-A activity, elevated mitochondrial membrane potential, and sensitivity to F16. Our results show that suppressing aerobic lactate production directly impacts mitochondrial respiration. Cells with decreased LDH-A activity showed an increase in oxygen consumption and OXPHOS activity. The $\Delta\psi_m$ was significantly lower in the knockdown clones, and the accumulation of F16 in the organelles of these cells was markedly diminished. In addition, the tumorigenic potential of the malignant cells was severely compromised by LDH-A knockdown. Ectopic expression of human LDH-A restored the glycolytic capacity of the LDH-A knockdown cells, and this event was sufficient to reverse the phenotypes observed in vitro and in vivo. Altogether, the results indicate that alterations in glucose metabolism in transformed cells are tied to a reorganization of mitochondrial physiology. Furthermore, the data are consistent with the role of LDH-A as an essential tumor maintenance gene and provide further support to the concept of inhibition of glucose metabolism as an attractive antitumor strategy.

Results

Isolation of tumor cell lines with stable knockdown of LDH-A

Sensitivity to glucose deprivation as well as elevated LDH-A activity has been well documented in a variety of human breast cancer cell lines and tissue sections, respectively (Aft et al., 2002; Balinsky et al., 1983). The glucose dependency and LDH-A activity are shown for *neu*-initiated mammary epithelial tumor cell lines in which a higher than normal $\Delta\psi_m$ has been previously observed (Figures 1A and 1B). In comparison to immortalized, nontransformed mouse mammary epithelial EpH4, HC11, and NMuMg cells, all *neu*-initiated tumor cell lines were extremely sensitive to treatment with the anti-metabolite 2-deoxy-D-glucose, a well-characterized glucose antagonist, and displayed elevated LDH-A activity. Expression of short hairpin RNAs (shRNAs) complementary to LDH-A was used to stably suppress expression of the enzyme. Recombinant vectors containing oligonucleotide sequences encoding three shRNAs (L1, L2, and L3) under the U6 promoter were transfected into the *neu*-initiated tumor cells. We focused our efforts on Neu4145 and NF980 cell lines. These cells did not undergo apoptosis upon transient transfection of shRNA-expressing vectors. A series of stable clones with varying degrees of expression of LDH-A protein were isolated (Figure 1C). As previously reported for tumor cells, the expression of LDH-B protein was low in Neu4145 cells and was not affected in the derived knockdown cells (data not shown). The highest level of suppression of LDH-A protein was achieved by L2 and L1 hairpins. The knockdown was functionally assessed by LDH enzymatic assay (Figure 1D). There was good correlation between the LDH-A activity and LDH-A protein levels in the cell lines analyzed. Clones L2-5 and L2-10 showed a 69% and 75% reduction of LDH-A protein, and 60% to 70% reduction in enzyme activity, respectively.

LDH-A suppression affects growth properties of *neu*-initiated tumor cells

We next characterized the growth properties of parental and LDH-A knockdown clones under normal and limiting oxygen pressure (Figure 2). Under normoxic conditions, the rate of proliferation of cells with decreased LDH-A protein was retarded (Figure 2A). These observations showed the reliance of tumor cells on glycolysis under normal oxygen conditions. Unlike the parental Neu4145, growth of LDH-A-deficient tumor cells was severely affected under hypoxic conditions (0.5% oxygen) (Figure 2B). After 3 days from plating, the rates of proliferation of parental cells and their derivatives with decreased LDH-A activity differed by about 100-fold. To determine if the growth defect observed was a consequence of the inability of LDH-A-deficient *neu*-initiated tumor cells to metabolize glucose to lactate, the cDNA corresponding to human LDH-A was introduced into L2-5 cells (Figure 2C). As shown for clone L2-5.c15, ectopic expression of LDH-A restored the rate of proliferation under normal or low oxygen pressure conditions (Figures 2A and 2B). These results confirm the specificity of the LDH-A knockdown approach and ruled out off-target effects as responsible for the proliferation defect. The data are also in agreement with previous work that established an essential role for LDH-A in supporting anchorage-independent growth of c-Myc-transformed cells (Shim et al., 1997). To determine the impact of LDH-A knockdown on the cellular energy balance, ATP levels were measured under normal and low oxygen conditions (Figure 2D). In comparison to parental Neu4145 cells, a modest decrease (16%) in the ATP pool was detected in LDH-A-deficient L2-5 cells under normal pO_2. On the other hand, ATP levels were significantly lower (51%) in clones L2-5 and L2-10 under hypoxia (Figure 2D). Similar results were observed with NF980 tumor cells as well as derived LDH-A-deficient clones (Figures S1A–S1C in the Supplemental Data available with this article online). The inability of cells with decreased LDH-A activity to sustain high ATP levels most likely explains the block in proliferation under conditions of oxygen deprivation. The effect of LDH-A knockdown on the proliferation of immortalized, nontransformed mouse mammary epithelial EpH4 cells (Lopez-Barahona et al., 1995; Reichmann et al., 1989, 1992) was also monitored (Figure 2E). The EpH4 cells are fully polarized, nontumorigenic in nude mice, and capable of forming 3D tubular structures when grown in collagen gels, reminiscent of normal luminal epithelial cells (Fialka et al., 1996; Oft et al., 1996). The growth of both EpH4 and LDH-A-deficient subclone EpH4.L2-13 was indistinguishable under normal pO_2. Neither EpH4.L2-13 nor the parental EpH4 cells proliferated under hypoxia, in contrast to

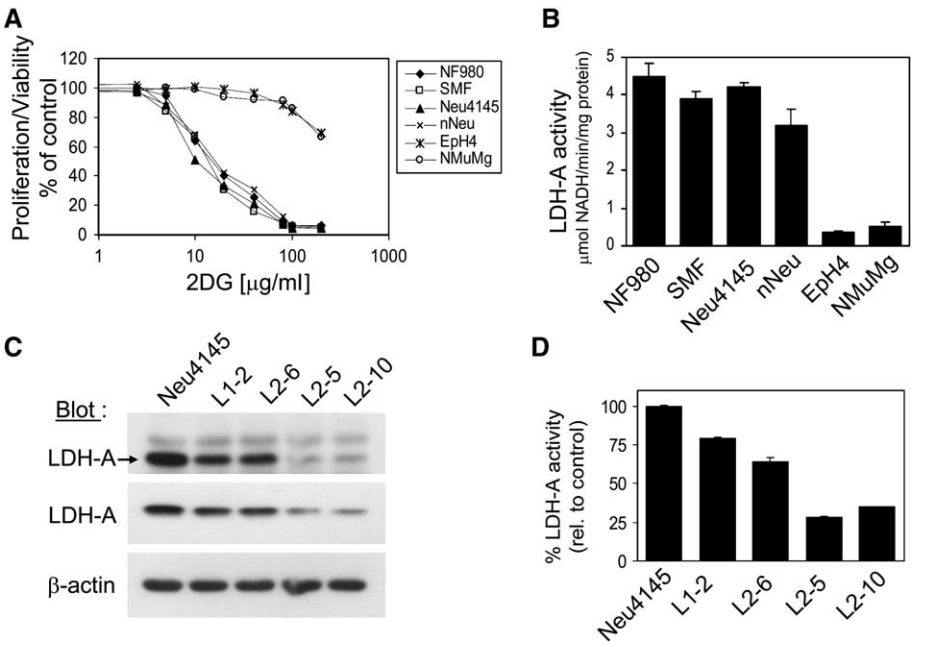

Figure 1. Characterization of glucose dependency and LDH-A activity of mouse mammary tumor cell lines

A: Neu-initiated tumor cell lines as well as immortalized nontransformed EpH4 and NMuMg cells were grown in the presence of increasing amounts of the glucose anti-metabolite 2-deoxy-D-glucose as indicated for 48 hr. Proliferation was assessed by BrdU-incorporation assay described under Experimental Procedures. Results were expressed as average percent ± SEM of vehicle-treated control.

B: Comparison of LDH-A activity across a panel of normal and tumor mouse mammary epithelial cell lines. The results represent the average ± SEM of three independent experiments.

C: Western blot analysis was performed on whole-cell lysates prepared from Neu4145 cells and selected clones stably expressing shRNAs for LDH-A. Samples were probed with goat polyclonal anti-LDH (top panel) and mouse monoclonal anti-LDH-A (middle panel). Membranes were reprobed with anti-β-actin as a loading control (bottom panel).

D: LDH-A activity in knockdown clones, expressed as percent of enzyme activity in parental Neu4145 cells.

the hypoxia tolerance of the tumor cell lines Neu4145 and NF980. Similar results were obtained in studies with nontransformed mammary epithelial HC11 cells (Figure S1D). This difference reflects the OXPHOS reliance of these nonmalignant lines and highlights the metabolic adaptation of malignant ones. Altogether, the results demonstrate that tumor cells rely on LDH-A activity even when oxygen is not limiting, and that endurance of tumor cells in a hypoxic environment is highly dependent on LDH-A activity.

Mitochondrial activity in tumor cells is affected by LDH-A knockdown

As mentioned earlier, we had reported the identification of F16, a delocalized lipophilic cation that is selectively toxic to carcinoma cells with elevated $\Delta\psi_m$. Mitochondrial membrane and plasma membrane hyperpolarization, the basis for the selectivity of F16 for carcinoma cells, have been described for a variety of malignant cells. However, to date there is no clear understanding for the basis of this phenomenon. Tumor cells in general exhibit reduced OXPHOS activity (Capuano et al., 1997; Cuezva et al., 2002; Isidoro et al., 2004). We and others have proposed that the increased rate of aerobic lactate production, the lower OXPHOS activity, and the elevated $\Delta\psi_m$ commonly observed in transformed cells could be interrelated phenomena. In principle, the inability of tumor cells to use mitochondria to meet their energetic demand, which coincides with dissipation of a smaller fraction of the mitochondrial proton gradient ($\Delta\mu H^+$) normally used to produce ATP, may contribute to the elevated mitochondrial membrane potential ($\Delta\psi_m$) observed in a variety of carcinoma cells. We reasoned that the inherently highly glycolytic Neu4145 cells, and derived clones with decreased LDH-A activity, could provide the perfect setting to test this model. We compared F16 accumulation, mitochondrial membrane potential, and respiration rate in Neu4145 cells and LDH-A knockdown clones. First, cells were incubated in medium containing 3 μM F16 (Figure 3A). In contrast to Neu4145 cells, no significant build-up of F16 in the mitochondria compartment was observed in LDH-A-deficient L2-5 and L2-10 cells. On the other hand, LDH-A complementation restored the ability of cells to accumulate F16 as depicted by clone L2-5.c15. The reduced accumulation of F16 in cells with LDH-A knockdown was confirmed by semiquantitative flow cytometric analysis (Table 1). No differences in mitochondrial morphology or mitochondrial volume density were observed by electron microscopy analysis of glutaraldehyde-fixed cells (Figure 3B). The mitochondrial mass across these cell lines was comparable as assessed by analysis of cells incubated with the mitochondrial cardiolipin dye nonyl-acridine orange (Table 1).

Next, to gain a clear insight into the adaptation of mitochondrial metabolism upon LDH-A knockdown, we performed a detailed bioenergetics analysis of mitochondrial functions in the four experimental cell lines described above. The rate of respiration was assessed by the measurement of oxygen consumption using a Clark-type electrode. First, it is important to appreciate that mitochondrial respiration consists of coupled and uncoupled respiration. Coupled respiration represents the fraction of mitochondrial respiration that is used for ATP production, while uncoupled respiration represents the fraction of mitochondrial respiration that is used to drive a futile cycle of protons across the biological membrane, called proton leak. The mitochondrial metabolic organization of cells represents the fraction of mitochondrial respiration that is used to drive proton leak and ATP turnover. On average, animals spend as much as 20% of their basal mitochondrial respiration to drive proton leak (Rolfe and Brown, 1997), and the remaining 80% is used for ATP turnover. Many physiological functions have been proposed for proton leak, but the two most prominent ones are for heat production and protection against reactive oxygen species. Reduction of LDH-A levels in the L2-5 and L2-10 clones resulted in an increase in total mitochondrial respiration compared with Neu4145 control cells (Figure 4A). The complementation of the L2-5 clone with LDH-A reduced the total mitochondrial respiration back to control levels. This increase in total mitochondrial respiration in the L2-5 and L2-10 clones was reflected in both

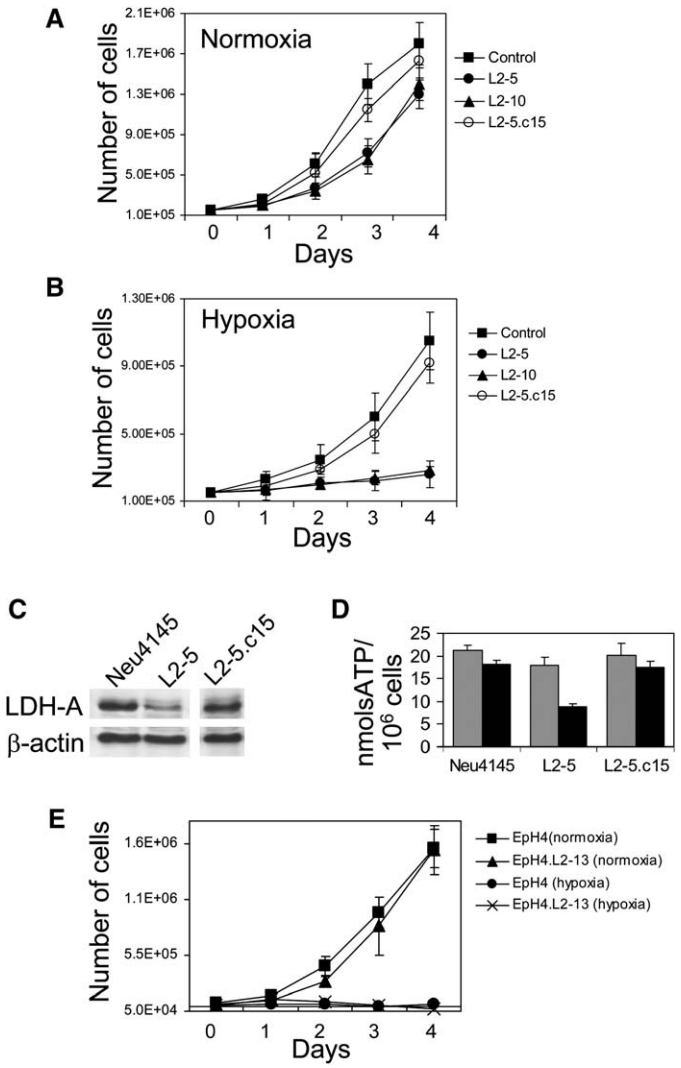

Figure 2. Effect of LDH-A knockdown on growth properties of tumor cells in vitro

A: Proliferation curve for parental Neu4145 tumor cells (control) and LDH-A-deficient clones L2-5 and L2-10 grown under normal oxygen pressure.
B: Proliferation curve for cells grown under hypoxic conditions. Ectopic expression of human LDH-A restores the ability of L2-5 clone to endure hypoxia.
C: Western blot analysis was performed on whole-cell lysates prepared from parental cells (Neu 4145), LDH-A-deficient cells (clone L2-5), and LDH-A-complemented cells (clone L2-5.c15) as described under Experimental Procedures. Equivalent amounts of proteins were immunoblotted with anti-LDH-A and β-actin as loading control.
D: Quantification of ATP levels in cells grown under normoxic (gray bars) and hypoxic (black bars) conditions for 48 hr using a luciferin-luciferase-based assay. Results represent the average ± SEM of three experiments.
E: Proliferation curve for immortalized, nontransformed EpH-4 cells and LDH-A-deficient cells (clone L2-13) under normal oxygen pressure and hypoxic conditions.
Results in **A**, **B**, and **E** represent the average ± SEM of two independent experiments.

ATP turnover (Figure 4B) and proton leak (Figure 4C). Indeed, the L2-5 and L2-10 clones displayed higher proton leak and ATP turnover than Neu4145 control cells. Again, the L2-5 complemented clone had low rates of proton leak and ATP turnover, similar to controls. Since the fold increase in proton leak and ATP turnover is similar in the two LDH-A knockdown clones, the metabolic organization of all four clones was similar (Figure 4D). Indeed, each clone devoted around 25% of its total mitochondrial respiration for proton leak and 75% for ATP turnover. The decrease in F16 accumulation and increase in respiration rate observed in L2-5 and L2-10 clones suggested that reduction in LDH-A activity is accompanied with a reduction in $\Delta\psi_m$. To show conclusively that knockdown of LDH-A is associated with a reduced $\Delta\psi_m$, we measured this parameter quantitatively using [^{3}H]triphenylmethylphosphonium (TPMP). In comparison to Neu4145 control cells, LDH-A knockdown L2-5 and L2-10 clones displayed lower $\Delta\psi_m$ (Table 2). Importantly, the L2-5.c15 clone complemented with LDH-A showed a mitochondrial membrane potential almost identical to that of Neu4145 cells.

One of the factors that affect the rate of respiration is NADH levels. Since the LDH-A-catalyzed conversion of pyruvate into lactate consumes NADH and regenerates NAD^+, next we investigated the cellular levels of both pyridine nucleotides. The ratio of free NADH/NAD^+ in the cytosol was estimated from the concentrations of pyruvate and lactate considered to be in near equilibrium with the couple. A 2-fold increase in the NADH/NAD^+ was measured in the L2-5 and L2-10 clones deficient in LDH-A (Table 2). The modest but reproducible difference indicated that LDH-A knockdown resulted in a perturbation in the cytosolic NADH and NAD^+ pools.

In conclusion, reduction of LDH-A levels resulted in increased cytosolic NADH/NAD^+, consistent with the increased respiration rate and elevated mitochondrial membrane potential. In addition, the metabolic organization of the Neu4145 control cells and knockdown clones were similar, an indication of the organelle's ability to respond both to substrate availability and cellular energetic demand and adapt its metabolic activity.

LDH-A suppression interferes with tumorigenicity of malignant cells

Downregulation of LDH-A activity had a profound impact on mitochondria bioenergetics and interfered with proliferation of Neu4145 tumor cells in culture. The well-established reliance of cancer cells on the glycolytic pathway, characterized by the increased production of lactate, may indicate that the high ATP demand of cancer cells cannot be solely fuelled by mitochondrial metabolism and/or that mitochondrial metabolism is somehow defective. It has been observed that in rodents LDH-A increases during mammary gland tumorigenesis (Richards and Hilf, 1972). LDH-A protein expression is higher in human breast tumor tissue compared to normal tissue, and in lung cancer LDH-A overexpression is a negative prognostic marker (Balinsky et al., 1983; Hilf et al., 1976; Koukourakis et al., 2003). These findings prompted us to address the role of LDH-A in tumorigenesis. We asked whether LDH-A knockdown that forced tumor cells to rely exclusively on ATP supplied by mitochondrial OXPHOS could affect their tumorigenic capacity. To this end, Neu4145 tumor cells and derived LDH-A knockdown clones were orthotopically transplanted into mammary gland fat pads of 6- to 8-week-old female mice, and tumor growth was monitored thereafter. The fact that the Neu4145 cell line was established from a mammary gland tumor excised from a *neu*-transgenic FVB female mouse enabled syngeneic transplantation of these cells as well as derived clones. The parental Neu4145 tumor cell line, LDH-A-deficient L2-5 cells, and LDH-A-complemented L2-5.c15 cells were injected into the fourth

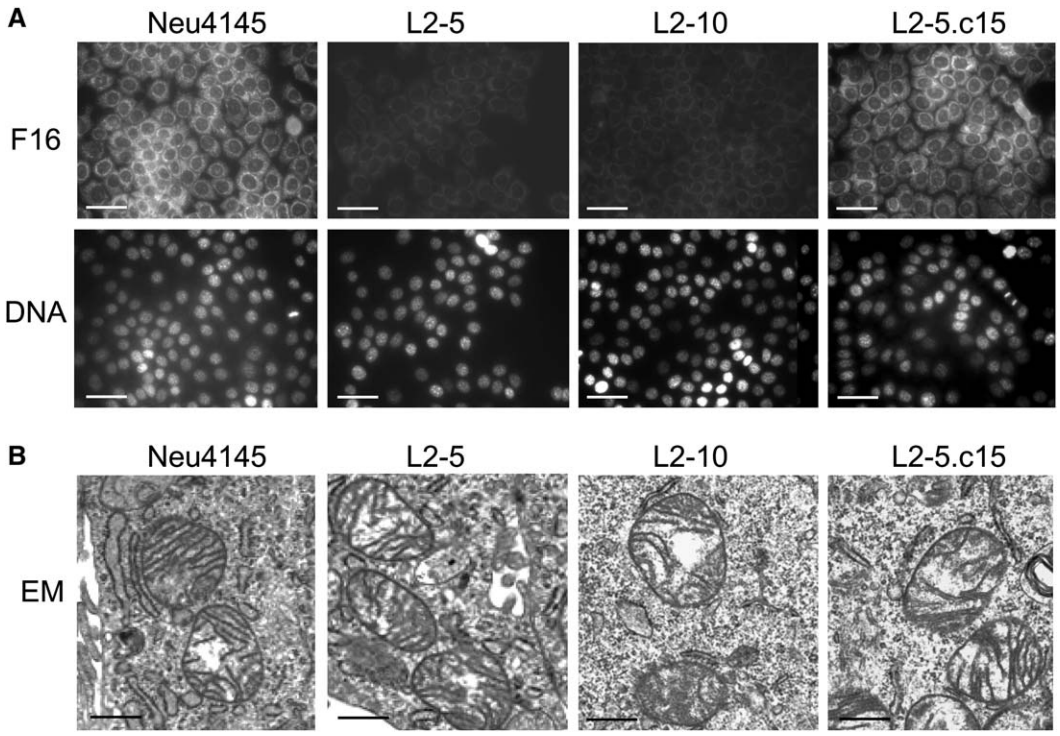

Figure 3. Effect of LDH-A knockdown on mitochondrial accumulation of the lipophilic cation

A: Cells were incubated with F16 as indicated under Experimental Procedures prior to imaging. Fluorescent F16 signal (top row) and DNA (bottom row). Scale bars, 50 μm.

B: Images of mitochondria obtained by electron microscopy from ultrathin cryosection prepared from parental Neu4145 and derived clones. Scale bars, 200 nm.

gland of female mice, and the three cohorts established were monitored weekly. Palpable tumors were evident 1 week after Neu4145 cell transplant. As depicted by the Kaplan-Meier survival plot, the first mouse bearing Neu4145-initiated tumors succumbed 42 days postinjection, at which point the average tumor volume for the cohort surpassed 1500 mm^3 (Figures 5A and 5B). By day 73 from initiation of the experiment, the complete cohort had passed. The median survival for the group with Neu4145-derived tumors was 58 days, that for the group with L2-5.c15-derived tumors was 64 days, and that for the group with L2-5-derived tumors was 162 days. The onset of tumor appearance and kinetics of tumor growth in the L2-5.c15 transplanted cohort was indistinguishable from that of the Neu4145-initiated group. In contrast, palpable nodules were not identified until 5 weeks postinjection in the L2-5-transplanted mice. The growth rate of these tumors was remarkably low when compared to that of Neu4145 and L2-5.c15 tumors. By 12 weeks postinjection, divergence in the tumor growth rate for two mice within the group became noticeable. The first mouse within this cohort died 112 days after cell transplant. A second mouse died at day 129. The experiment was terminated 4 months after initiation, at which point 80% of the L2-5.c15 cohort was still alive. Similar observations were made with a small cohort of mice bearing tumors derived from the NF980 tumor cell line and LDH-A-deficient subclone (Figures S2 and S3). In all cases, tumors were removed at necropsy and subjected to histologic examination. To assess proliferation, tumor sections were examined for the expression of the mitotic marker Ki67 (Figure 5C). A similar average in the number of Ki67-positive cells/100 tumor cells was observed for Neu4145 and LDH-A-complemented L2-5.c15-derived tumors (16% ± 2.2% and 17.4% ± 2.0%, respectively). In contrast, the number of cells positive for Ki67 (1.3% ± 0.9%) was markedly reduced in L2-5 derived tumors ($p < 0.03$), consistent with the slow growth of these tumors. In addition, the pockets of necrotic and scar tissue present in these small tumors were only comparable to those observed in the oversized Neu4145-derived tumors (Figure 6A). Tumors excised 3 weeks after injection of Neu4145 cells, with comparable size to those of L2-5-initiated tumors 14 weeks postinjection were primarily comprised of proliferating cells, indicating the inability of LDH-A knockdown cells to endure the tumor microenvironment and grow beyond small lesions. Western Blot analysis to examine LDH-A levels was performed on lysates prepared from the isolated tumors (Figure 6B). Whole-cell lysates were prepared from cell suspensions enriched for *neu*-initiated tumor cells following fractionation, to minimize the contribution of nontumor cell types present in the samples. LDH-A expression was homogenously low among

Table 1. Comparison of F16 accumulation and NAO staining by flow cytometry

Cell line	F16 accumulation: log F16 emission (a.u.)	Mitochondrial mass: NAO ratio, 630 nm/530 nm
Neu4145	218 ± 15.2	2.44
L2-5	45 ± 2.9	2.65
L2-10	52 ± 3.8	2.53
L2-5.c15	196 ± 8.3	2.39

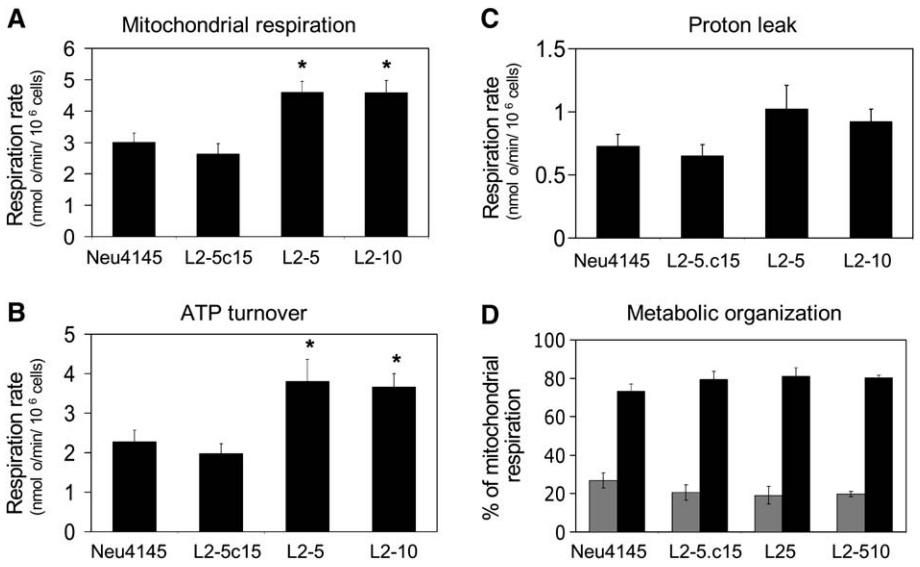

Figure 4. Bioenergetic analysis of Neu4145 parental tumor cells, derived LDH-A-deficient L2-5 and L2-10 clones, and LDH-A-complemented L2-5.c15 clone

A: Total mitochondrial respiration consists of ATP turnover and proton leak.

B: ATP turnover represents the respiration that is sensitive to the inhibitor of the ATP synthase, oligomycin.

C: Proton leak represents the respiration that is insensitive to oligomycin.

D: Metabolic organization is the fraction of mitochondrial respiration that is used for ATP turnover (black bars) and proton leak (gray bars).

The experimental conditions are defined in Experimental Procedures. Results are expressed as average ± SEM. Statistical significance is indicated with an asterisk ($p \leq 0.05$). Data were subjected to one-way ANOVA and a posteriori Tukey test.

tumors in the L2-5 group with the exception of samples prepared from the two outlier animals within the cohort. It is likely that silencing of the U6 promoter driving the expression of the shRNA could account for the restoration of LDH-A levels in these tumors. But regardless of the mechanism for restoration of LDH-A expression in these tumors, these results further link LDH-A expression with tumor proliferation and emphasize the essential role of glycolysis for malignant growth.

Discussion

In the present study, we asked whether the high rate of glycolysis was an essential tumor phenotype and whether there was a link between this phenomenon and the widely described alterations in mitochondrial metabolism in tumor cells. To this end, we utilized shRNAs to downregulate the expression of LDH-A in *neu*-initiated mammary tumor cells, and to interfere with the ability of cells to convert glucose-derived pyruvate into lactate. Our results show that this shift in metabolic strategy upon LDH-A knockdown had a drastic impact on tumor physiology. The data also provide evidence that indeed the alterations in mitochondrial membrane potential are a consequence of the "glycolytic phenotype" essential for tumor growth.

Although the conversion of pyruvate into lactate occurs in normal cells in hypoxic conditions, tumor cells produce copious amounts of lactate even when oxygen is not a limiting factor. It has been proposed that this phenotype results from the adaptation of premalignant lesions to intermittent hypoxia (Gatenby and Gillies, 2004). However, the molecular mechanisms leading to the increased rate of glycolysis are only partially understood.

Table 2. Mitochondrial membrane potential and NADH/NAD$^+$ of parental Neu4145 tumor cells and derived clones

Cell line	Mitochondrial membrane potential (mV)	Free NADH/NAD$^+$
Neu4145	209.2 ± 2.5	3.7×10^{-3}
L2-5	185.5 ± 2.9	5.8×10^{-3}
L2-10	178.2 ± 2.4	5.5×10^{-3}
L2-5.c15	207.1 ± 2.4	3.2×10^{-3}

Our results show that limiting the LDH-A activity of several tumor cell lines is sufficient to stimulate OXPHOS in these cells, evidence of the direct link between these two processes. It is important to emphasize though that the reversion from a highly glycolytic metabolism to an OXPHOS-based metabolism was only achieved by a subset of the tumor cell lines studied. Some tumor cells had a strict LDH-A requirement. Because tumors arise through a Darwinian evolutionary process, the selected glycolytic phenotype could emerge as a consequence of one or multiple reversible and/or irreversible adaptations that confer a growth advantage. It is likely that the oxidative phosphorylation capacity of some of these tumor cell lines had been irreversibly diminished as previously described (Capuano et al., 1997; Cuezva et al., 2002; Isidoro et al., 2004).

In comparison to parental tumor cells, those clones with decreased LDH-A activity that are still capable of proliferating under normoxia exhibited a severe growth defect under hypoxic conditions in vitro. Previous work has shown that overexpression of LDH-A alone is not sufficient to induce malignant transformation (Lewis et al., 2000). However, the LDH-A dependency of Myc-transformed cells for in vitro proliferation under anaerobic conditions as well as for soft agar clonogenicity has been clearly established (Shim et al., 1997). Our results showed that LDH-A deficiency significantly compromised the tumorigenic potential of *neu*-initiated tumor cells transplanted into mice. At the cellular level, limiting LDH-A activity led to an increase in the rate of oxygen consumption, which was accompanied by a decrease in mitochondrial membrane potential. LDH-A-deficient cells failed to significantly accumulate the lipophilic cation F16, which preferentially concentrates in cells with elevated mitochondrial membrane potential. Using the opposite approach, it has been observed that acute LDH-A overexpression in pancreatic β cells results in an increase in mitochondrial membrane potential (Ainscow et al., 2000). These results, like ours, highlight the fine interplay that exists between glycolysis and mitochondrial metabolism. Both LDH-A and mitochondria activity are mutually regulated at the level of metabolites. They depend on the availability of pyruvate and on the NADH/NAD$^+$ ratio. In the presence of oxygen, ATP is generated by oxidation of pyruvate in the mitochondria. Alternatively, ATP can be generated by

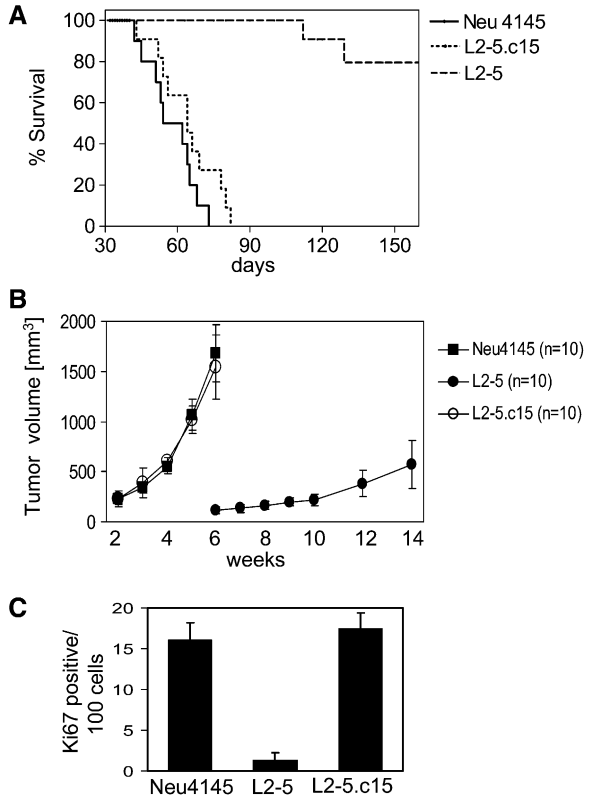

Figure 5. Characterization of growth properties of LDH-A-deficient tumors

Parental Neu4145, LDH-A-deficient L2-5, and complemented L2-5.c15 cells were injected into the 4th gland mammary fat pad as described under Experimental Procedures.

A: Kaplan-Meier survival plot for the three cohorts (ten mice per group). The probability of survival was significantly higher for the group with tumors derived from LDH-A-deficient L2-5 cells (Kaplan-Meier, chi-square = 44.96, df = 2; log-rank $p < 0.0001$).

B: Kinetics of tumor growth.

C: Number of cells that scored positive for the mitotic marker Ki67, expressed on a percent basis.

For **B** and **C**, results are expressed as average ± SD.

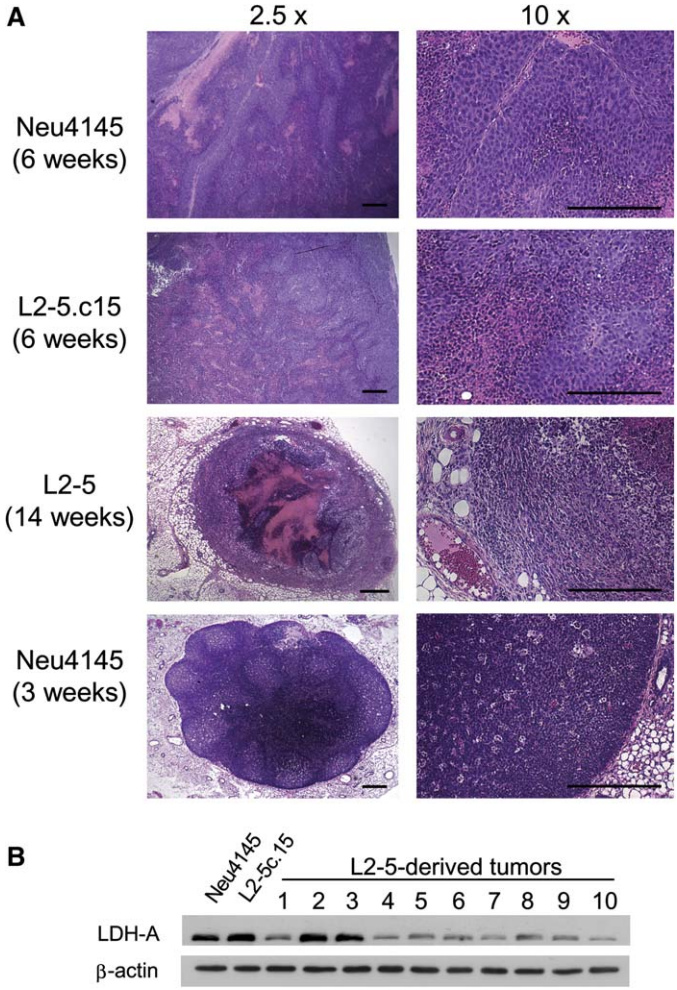

Figure 6. Histology and characterization of LDH-A expression in tumors

A: Tumors derived from Neu4145, L2-5, and L2-5.c15 cell transplants were removed at time of necropsy, fixed, and subjected to H&E staining. The smaller size of LDH-A-deficient lesions is evident in the images on the left column taken at identical magnification (corresponding 10× magnification images are shown on the right column). For a comparison of relative size, tumors derived from Neu4145 transplants were dissected 3 weeks postinjection with volume comparable to that of L2-5-derived tumors approximately 14 weeks postinjection. Scale bars, 200 μm.

B: Western blot analysis of LDH-A expression of tumor whole-cell lysates prepared as described under Experimental Procedures. Samples were probed for β-actin as a loading control.

conversion of glucose to lactate in the cell cytoplasm. In this case, NADH-dependent LDH-A catalyzes the conversion of pyruvate into lactate. A number of factors may contribute to the preferential funneling of pyruvate to lactate in transformed cells. As mentioned earlier, higher levels of glycolytic enzymes and alterations in isoenzyme types are commonly observed in cancer cells. Furthermore, reduced capacity to transport cytosolic NADH into mitochondria has been reported in rapidly proliferating cells (Greiner et al., 1994). The fast kinetics of LDH-A-catalyzed conversion of pyruvate into lactate ensures rapid and constant supply of ATP but rapidly consumes NADH. Thus, LDH-A regenerates NAD^+ in the cytoplasm and competes with the mitochondrial NADH/NAD^+ shuttle systems (Golshani-Hebroni and Bessman, 1997). The LDH-A competition for NADH is most likely at the core of the slowdown of mitochondrial respiration. In addition, as a consequence of the elevated lactate production, the decrease in cytoplasmic pH will also impact the efficiency of the OXPHOS chain (Conley et al., 2001). As previously proposed for proliferating T lymphocytes, it is also likely that the overall higher rate of glycolysis causes a net increase in the proportion of ADP bound to glycolytic enzymes. This may establish a competition for the nucleotide diphosphate between these enzymes and the mitochondrial nucleotide translocator ANT (Brand, 1997).

The deviation from cellular metabolic homeostasis has been exploited for cancer diagnosis. The differential mitochondrial membrane potential of malignant cells plays a role in the selective accumulation of cationic, lipophilic ^{99m}Tc complexes used for tumor imaging. The heavy glucose reliance of tumor cells constitutes the basis for tumor imaging by positron emission tomography. These same alterations are beginning to emerge as selective tumor traits that could provide the basis for novel therapeutic approaches. The higher potential across the inner mitochondrial membrane of carcinoma cells serves a selective driving force for the accumulation of toxic delocalized lipophilic

cations like dequalinium, MKT-077, and F16 (Costantini et al., 2000; Fantin et al., 2002; Modica-Napolitano and Aprille, 2001). The use of the anti-metabolite 2-deoxy-D-glucose to antagonize the high glucose dependency of tumors has been evaluated in vitro as a potential novel chemotherapeutic approach for the treatment of cancer (Aft et al., 2002). Based on the observed strong LDH-A dependency for tumor proliferation from both in vitro and in vivo studies, we propose that inhibition of LDH-A may represent an alternative strategy toward the development of anti-glycolytic-based therapeutic strategies for the treatment of cancer. The tumor dependency on the glycolytic pathway activity could arise as a consequence of genetic alterations or could be a selected metabolic strategy based on metabolite control with no underlying genetic defects. These metabolic adaptations are essential to confer cells with full tumorigenic potential. Our results from the in vivo experiments demonstrate that tumors rely on glucose to lactate conversion for growth, and that interfering with this process restricts the ability of tumor cells to grow beyond small lesions. LDH-A activity is upregulated in tumors, and it constitutes a bottleneck for malignant cells proliferating in the extreme tumor microenvironment. Complete lack of LDH-A subunit production has been identified in humans (Kanno et al., 1988). Individuals with hereditary LDH-A deficiency show myoglobinuria only after intense anaerobic exercise (exertional myoglobinuria) but do not show any symptoms under ordinary circumstances. Altogether, our results and the literature suggest that antagonizing LDH-A may be in principle achievable, tolerated, and an effective antitumor approach.

Finally, the integration of information derived from genetic approaches like the one utilized here and more global small molecule-based "perturbational profiling" strategies (Ramanathan et al., 2005) may prove powerful in providing complementary tools to better dissect the essential metabolic alterations that give rise to the cancer metabolic phenotype.

Experimental procedures

Reagents

Goat polyclonal anti-LDH-A was purchased from Chemicon and anti-β-actin from Sigma. F16 was obtained from Asinex, Hoechst 33342 from Molecular Probes, and 2-deoxy-D-glucose from Sigma. Purified mouse monoclonal anti-LDH-A was a generous gift of Dr. Yves Charnay (Geneva University Hospitals, Geneva, Switzerland). LDH-A-derived DNA oligonucleotides encoding shRNA were purchased from Qiagen, Inc. The pSG5 containing the human LDH-A cDNA was obtained from Dr. Chi V. Dang's laboratory (Johns Hopkins University School of Medicine) and pSHAG from Dr. Gregory Hannon's laboratory (Cold Spring Harbor Laboratory).

Cell culture and generation of stable cell lines

Unless indicated, cells were grown in Dulbecco's modified Eagle's medium (DMEM), 10% FBS at 37°C/5% CO_2. For experiments performed under hypoxic conditions, cells were grown in the same medium supplemented with 25 mM HEPES, in a modular chamber (Billups-Rothenberg Inc.). The gas flow was controlled by a single flow meter (Billups-Rothenberg Inc.). The hypoxic chamber was equilibrated with a gas mixture containing 0.5% O_2/5% CO_2/94.5% N_2 for 15 min prior to being sealed. NMuMg were obtained from the ATCC. The tumor cell lines nNeu, NF980, SMF, NAF, and Neu4145 have been established in our laboratory from mammary gland tumors dissected from *neu*-transgenic mice. Immortalized, nontransformed mouse mammary epithelial EpH4 cells were obtained from Dr. Hartmut Beug (Research Institute of Molecular Pathology, Vienna, Austria).

Stable expression of shRNAs from the U6 promoter in pSHAG-1 vector in mouse tumor cell lines was achieved following the BseRI-BamHI protocol (http://katahdin.cshl.org/homepage/portal/scripts/main2.pl?link=protocols&content=protocols.html). Design of three shRNA inserts for pSHAG-1 vector, containing a 29-base stem structure complementary to the LDH-A (Genbank NM_010699) was done by software found in Dr. Gregory Hannon's laboratory website (http://www.cshl.edu/public/SCIENCE/hannon.html). The selected oligonucleotide sequences corresponding to nt 204–232 (L1), nt 737–765 (L2), and nt 1161–1188 (L3) did not show significant homology to other murine sequences as determined by BLAST. Annealed and phosphorylated oligonucleotides were introduced into pSHAG-1 cleaved with BseRI and BamH1 (Paddison et al., 2002). The recombinant vector was linearized with EcoRV and cotransfected with pPur (Clontech) using Fugene 6 Reagent according to the manufacturer's protocol (Roche). Selection of stable clones was done in medium containing puromycin (1.5 μg/ml).

Proliferation assay

The effect of 2-deoxy-D-glucose on the proliferation of a panel of tumor cell lines was assessed by BrdU incorporation assay. Neu-initiated tumor cell lines n-Neu, NF980, SMF, NAF, and Neu4145, as well as immortalized, nontransformed mammary epithelial cell lines EpH4 and HC11, were resuspended in glucose-free DMEM medium supplemented with 5% dialyzed fetal bovine serum (90 mg/dl glucose, Invitrogen), 2 mM glucose, and 1 mM pyruvate. The cells were seeded in 384-well plates (2000 cells/50 μl) in the absence or in the presence of the indicated concentration of 2-deoxy-D-glucose and incubated for 36 hr. The cells were next subjected to a BrdU pulse (20 μM for 4 hr) followed by chemiluminescent anti-BrdU immunodetection as previously described (Fantin et al., 2002; Stockwell et al., 1999).

Determinations were done in triplicate, and the entire experiment was repeated twice.

LDH activity assay

Total LDH-A activity was compared across clones as previously described (Sekine et al., 1994). Briefly, 5×10^6 cells were resuspended in 500 μl assay buffer and sonicated (setting 5, twice 5 s). Enzyme and protein assay (Bradford, Bio-Rad) were performed on the supernatants obtained after centrifugation at 10,000 × g for 10 min (4°C). LDH-A activity was determined by monitoring the rate of NADH (20 μM) consumption upon addition of 2 mM pyruvate using a LS-50B spectrofluorometer (ex. 340 nm; em. 460 nm). Results from three experiments were normalized to protein content, averaged, and in some cases expressed as percent of LDH-A activity in parental Neu4145 cells.

Measurement of ATP

ATP levels were determined by luciferin-luciferase-based assay. Cells were grown under normal or 0.5% O_2 for 48 hr, harvested, and counted. Aliquots containing equal number of cells were processed using the ATP Bioluminescence Assay kit (Roche) according to standard protocol. Measurements were done in triplicate.

Lysate preparation and immunoblotting

Cells grown in tissue culture plates were rinsed with phosphate buffer saline (PBS) and lysed in Laemmli sample buffer containing Complete protease inhibitor cocktail (Roche). DNA was sheared by sonication for 5 s on ice. Protein concentration was determined by Lowry assay (Bio-Rad). Protein lysates were prepared from tumor samples following a simple fractionation protocol to enrich the cell suspension for HER-2-overexpressing tumor cells. One-half of the tumors removed were washed in Hank's balanced salt solution, weighed, and transferred to a plate containing DMEM (1:4 weight to volume). Tumors were minced with flat tip tweezers and dissociated in DMEM supplemented with 0.15% collagenase (Roche) for 3 hr. The cell suspension was centrifuged at 1000 rpm for 5 min in a tabletop centrifuge. The cell pellet was washed 3× with PBS and was resuspended in an appropriate volume of PBS/0.5% BSA that leaves 5×10^6 cells/ml. The cell suspension (0.5 ml) was incubated for 15 min on ice with 50 μl of anti-HER-2 coupled to Dynabeads (previously prepared by incubating 10 μl of rabbit polyclonal anti-HER2/Neu [Upstate Biotechnology] with 40 μl prewashed anti-rabbit Dynabeads M-280 IgG for 2 hr on ice following standard procedure [Dynal Biotech]). The complex (cells bound to anti-HER-2/anti-rabbit-Dynabeads) was captured with the magnet, washed 3× with PBS, and resuspended in 200 μl of Laemmli sample buffer. DNA was sheared by sonication as previously indicated. Protein concentration was determined by Lowry assay.

An aliquot of each lysate containing equivalent amounts of protein was separated by SDS-PAGE and transferred to Immobilon-P membranes (Millipore) in buffer consisting of 25 mM Tris, 190 mM glycine, 20% methanol, 0.005% SDS. Membranes were blocked with 1.5% BSA in TBST (150 mM NaCl, 20 mM Tris-HCl [pH 7.4], 0.3% Tween 20). Primary antibodies and secondary antibodies were diluted in the same buffer containing 0.2% BSA. Membranes were washed with TBST buffer and developed with horseradish peroxidase conjugated to anti-mouse IgG (Amersham) or to anti-goat IgG (Southern Biotechnology). The enhanced chemiluminescence reagent (Pierce) was used for detection.

Localization of F16 in living cells

Cells were seeded in 4-well chamber slides 16 hr prior to treatment. Cells were left untreated or were treated with 3 μM F16 for 3 hr at 37ºC. To stain nuclei DNA, Hoechst was added to the medium (1 μg/ml; Molecular Probes) and incubated for 30 min at 37ºC prior to imaging. The fluorescent signal of F16 was visualized using a standard fluorescein filter set. Cells were photographed under Axioskop microscope using a Spot Camera (Diagnostic Instruments). Magnification: 10×.

Flow cytometry

The ability of cells to accumulate the fluorescent delocalized lipophilic cation F16 (abs. 420 nm/em. 520 nm) was compared by flow cytometry. Cells were incubated for 1 hr in medium containing 1 μM F16, harvested, washed with PBS, resuspended in growth medium, and immediately analyzed. Measurements were done in triplicate. To compare mitochondrial mass, cells were incubated with the cardiolipin stain nonyl-acridine orange (NAO, Molecular Probes). Cells were stained and analyzed as previously described (Fantin et al., 2002). Results represent the average of two independent experiments.

Electron microscopy

Cells grown in 35 mm dishes were fixed for 1 hr at room temperature in 0.1 M Cacodylate buffer containing 1.25% formaldehyde, 2.5% glutaraldehyde, and 0.3% picric acid. Samples were then treated with 1% osmium tetroxide/1.5% potassium ferrocyanide, followed by 1% uranyl acetate, dehydrated, and epon-araldite embedded. Ultrathin sections were examined using a JEOL 1200EX microscope.

Respiration

Cells were resuspended in PBS supplemented with 25 mM glucose, 1 mM pyruvate, and 2% BSA. Cellular respiration was measured using a Clark-type oxygen electrode. In order to determine respiration that is used to drive proton leak and ATP turnover, cells were incubated in the presence of oligomycin (2.5 μg/10^6 cells). The respiration that is sensitive to oligomycin represents ATP turnover, while the respiration that is insensitive to oligomycin indicates proton leak. Determinations were done in quadruplicate, and the entire experiment was done twice.

Membrane potential measurements

Membrane potential measurements were carried out as described in Brand (1995). Basically, cells were incubated for 30 min with 0.2 μCi [3H]triphenylmethylphosphonium (TPMP), 0.2 μM TPMP, and 1.5 μM tetraphenylboron as carriers. To calculate membrane potential values, we used mitochondrial volume density of 8%, cell volume of 1 μl/10^6 cells, resting plasma membrane potential of −69 mV, and the following TPMP binding corrections: external medium, 0.7; cytoplasmic, 0.2; and mitochondrial, 0.4. Determinations were done in triplicate, and the entire experiment was done twice.

Determination of NADH/NAD^+ ratio

Cells grown in tissue culture plates were rinsed twice with PBS. Following addition of 1 ml of ice-cold perchloric acid (0.3 N), cells were removed with scraper. Insoluble material was removed by centrifugation, and aliquots of neutralized supernatant were used to measure pyruvate and lactate enzymatically as previously described (Bergmeyer, 1984). The free NADH/NAD^+ ratios were calculated from the lactate/pyruvate ratios using the equilibrium constant for LDH of 1.1×10^{-4} (at 28ºC) and pH = 7.

Syngeneic orthotopic transplant of tumor cell lines

Parental Neu 4145 cells, as well as derived clones Neu4145 L2-5 and Neu 4145 L2-5.c15, were resuspended at 0.5×10^6 cells/100 μl in PBS and injected into the fourth mammary gland fat pad of 6- to 8-week-old FVB female mice (Taconic Farms). For each cell line, a total of ten mice were injected. Mice were followed for survival analysis. Tumors were measured weekly with a caliper, and tumor volume was calculated using the following formula: volume (mm^3) = $width^2 \times length/2$. All animal studies were approved by the Institutional Animal Care and Use Committee (IACUC) at Harvard Medical School. Kaplan-Meier survival plot and statistical analysis were done with GraphPad Prism software. Statistical significance was determined using log-rank test.

Immunohistochemistry

Tumors were dissected at time of necropsy and cut in halves. One-half was utilized for protein lysates preparation, and the other half was rinsed in PBS and fixed in 10% paraformaldehyde/PBS. Samples were dehydrated in 70% ethanol, paraffin embedded, and sectioned (5 μm). Deparaffinized sections were stained for Ki67 antigen to assess proliferation. Briefly, samples were treated with 3% H_2O_2 at −20ºC for 10 min to neutralize endogenous peroxidase activity. Sections were then blocked in 5% BSA and incubated with rat anti-mouse Ki67 antibody (1:400 dilution; DAKO Corp.), followed by biotinylated rabbit anti-mouse IgG (1:200 dilution; Vector Laboratories). Detection was done with avidin-biotin-HRP complex (Vector laboratories) and di-aminobenzidine as chromogen. Nuclei were counterstained with hematoxylin. Ki67-positive cells were counted in four fields per tumor sample. Results are expressed as the average ± SD of five tumors per group.

Supplemental data

The Supplemental Data include three supplemental figures and can be found with this article online at http://www.cancercell.org/cgi/content/full/9/6/425/DC1/.

Acknowledgments

Our gratitude goes to Dr. Marcelo J. Berardi for his insightful advice. We also thank Dr. Roderick Bronson for expert help with histopathology and Maria Ericsson for assistance with electron microscopy. Montserrat Michelman provided help with screening and maintenance of stable clones, and Fen Zhou provided assistance with tissue culture.

Received: November 21, 2005
Revised: February 27, 2006
Accepted: April 24, 2006
Published: June 12, 2006

References

Aft, R.L., Zhang, F.W., and Gius, D. (2002). Evaluation of 2-deoxy-D-glucose as a chemotherapeutic agent: mechanism of cell death. Br. J. Cancer *87*, 805–812.

Ainscow, E.K., Zhao, C., and Rutter, G.A. (2000). Acute overexpression of lactate dehydrogenase-A perturbs β-cell mitochondrial metabolism and insulin secretion. Diabetes *49*, 1149–1155.

Balinsky, D., Platz, C.E., and Lewis, J.W. (1983). Isozyme patterns of normal, benign, and malignant human breast tissues. Cancer Res. *43*, 5895–5901.

Brand, M. (1995). Chapter 3: Measurement of mitochondrial protonmotive force. In Bioenergetics—A Practical Approach, G. Brown and C. Cooper, eds. (Oxford: Oxford University Press), pp. 39–62.

Bergmeyer, H.U. (1984). In Methods of Enzymatic Analysis, J. Bergmeyer and M. Graßl, eds. (Weinheim, Germany: Verlag Chemie), pp. 570–588.

Brand, K. (1997). Aerobic glycolysis by proliferating cells: protection against oxidative stress at the expense of energy yield. J. Bioenerg. Biomembr. *29*, 355–364.

Brand, K.A., and Hermfisse, U. (1997). Aerobic glycolysis by proliferating cells: a protective strategy against reactive oxygen species. FASEB J. *11*, 388–395.

Capuano, F., Guerrieri, F., and Papa, S. (1997). Oxidative phosphorylation enzymes in normal and neoplastic cell growth. J. Bioenerg. Biomembr. *29*, 379–384.

Chen, L.B. (1988). Mitochondrial membrane potential in living cells. Annu. Rev. Cell Biol. *4*, 155–181.

Conley, K.E., Kemper, W.F., and Crowther, G.J. (2001). Limits to sustainable muscle performance: interaction between glycolysis and oxidative phosphorylation. J. Exp. Biol. *204*, 3189–3194.

Costantini, P., Jacotot, E., Decaudin, D., and Kroemer, G. (2000). Mitochondrion as a novel target of anticancer chemotherapy. J. Natl. Cancer Inst. *92*, 1042–1053.

Cuezva, J.M., Krajewska, M., de Heredia, M.L., Krajewski, S., Santamaria, G., Kim, H., Zapata, J.M., Marusawa, H., Chamorro, M., and Reed, J.C. (2002). The bioenergetic signature of cancer: a marker of tumor progression. Cancer Res. *62*, 6674–6681.

Dang, C.V., and Semenza, G.L. (1999). Oncogenic alterations of metabolism. Trends Biochem. Sci. *24*, 68–72.

Dorward, A., Sweet, S., Moorehead, R., and Singh, G. (1997). Mitochondrial contributions to cancer cell physiology: redox balance, cell cycle, and drug resistance. J. Bioenerg. Biomembr. *29*, 385–392.

Fantin, V.R., Berardi, M.J., Scorrano, L., Korsmeyer, S.J., and Leder, P. (2002). A novel mitochondriotoxic small molecule that selectively inhibits tumor cell growth. Cancer Cell *2*, 29–42.

Fialka, I., Schwarz, H., Reichmann, E., Oft, M., Busslinger, M., and Beug, H. (1996). The estrogen-dependent c-JunER protein causes a reversible loss of mammary epithelial cell polarity involving a destabilization of adherens junctions. J. Cell Biol. *132*, 1115–1132.

Gatenby, R.A., and Gillies, R.J. (2004). Why do cancers have high aerobic glycolysis? Nat. Rev. Cancer *4*, 891–899.

Golshani-Hebroni, S.G., and Bessman, S.P. (1997). Hexokinase binding to mitochondria: a basis for proliferative energy metabolism. J. Bioenerg. Biomembr. *29*, 331–338.

Greiner, E.F., Guppy, M., and Brand, K. (1994). Glucose is essential for proliferation and the glycolytic enzyme induction that provokes a transition to glycolytic energy production. J. Biol. Chem. *269*, 31484–31490.

Heerdt, B.G., Houston, M.A., Wilson, A.J., and Augenlicht, L.H. (2003). The intrinsic mitochondrial membrane potential (Deltapsim) is associated with steady-state mitochondrial activity and the extent to which colonic epithelial cells undergo butyrate-mediated growth arrest and apoptosis. Cancer Res. *63*, 6311–6319.

Hilf, R., Rector, W.D., and Orlando, R.A. (1976). Multiple molecular forms of lactate dehydrogenase and glucose 6-phosphate dehydrogenase in normal and abnormal human breast tissues. Cancer *37*, 1825–1830.

Isidoro, A., Martinez, M., Fernandez, P.L., Ortega, A.D., Santamaria, G., Chamorro, M., Reed, J.C., and Cuezva, J.M. (2004). Alteration of the bioenergetic phenotype of mitochondria is a hallmark of breast, gastric, lung and oesophageal cancer. Biochem. J. *378*, 17–20.

Kanno, T., Sudo, K., Maekawa, M., Nishimura, Y., Ukita, M., and Fukutake, K. (1988). Lactate dehydrogenase M-subunit deficiency: a new type of hereditary exertional myopathy. Clin. Chim. Acta *173*, 89–98.

Koukourakis, M.I., Giatromanolaki, A., and Sivridis, E. (2003). Lactate dehydrogenase isoenzymes 1 and 5: differential expression by neoplastic and stromal cells in non-small cell lung cancer and other epithelial malignant tumors. Tumour Biol. *24*, 199–202.

Lewis, B.C., Prescott, J.E., Campbell, S.E., Shim, H., Orlowski, R.Z., and Dang, C.V. (2000). Tumor induction by the c-Myc target genes rcl and lactate dehydrogenase A. Cancer Res. *60*, 6178–6183.

Liang, B.C., Miller, L., and Weller, A. (1999). Ethyl-nitrosourea transformed astrocytes exhibit mitochondrial membrane hyperpolarization and constrained apoptosis. Apoptosis *4*, 89–97.

Lopez-Barahona, M., Fialka, I., Gonzalez-Sancho, J.M., Asuncion, M., Gonzalez, M., Iglesias, T., Bernal, J., Beug, H., and Munoz, A. (1995). Thyroid hormone regulates stromelysin expression, protease secretion and the morphogenetic potential of normal polarized mammary epithelial cells. EMBO J. *14*, 1145–1155.

Mathupala, S.P., Rempel, A., and Pedersen, P.L. (1997). Aberrant glycolytic metabolism of cancer cells: a remarkable coordination of genetic, transcriptional, post-translational, and mutational events that lead to a critical role for type II hexokinase. J. Bioenerg. Biomembr. *29*, 339–343.

Mazurek, S., and Eigenbrodt, E. (2003). The tumor metabolome. Anticancer Res. *23*, 1149–1154.

Modica-Napolitano, J.S., and Aprille, J.R. (2001). Delocalized lipophilic cations selectively target the mitochondria of carcinoma cells. Adv. Drug Deliv. Rev. *49*, 63–70.

Oft, M., Peli, J., Rudaz, C., Schwarz, H., Beug, H., and Reichmann, E. (1996). TGF-β1 and Ha-Ras collaborate in modulating the phenotypic plasticity and invasiveness of epithelial tumor cells. Genes Dev. *10*, 2462–2477.

Paddison, P.J., Caudy, A.A., Bernstein, E., Hannon, G.J., and Conklin, D.S. (2002). Short hairpin RNAs (shRNAs) induce sequence-specific silencing in mammalian cells. Genes Dev. *16*, 948–958.

Plas, D.R., and Thompson, C.B. (2002). Cell metabolism in the regulation of programmed cell death. Trends Endocrinol. Metab. *13*, 75–78.

Ramanathan, A., Wang, C., and Schreiber, S.L. (2005). Perturbational profiling of a cell-line model of tumorigenesis by using metabolic measurements. Proc. Natl. Acad. Sci. USA *102*, 5992–5997.

Reichmann, E., Ball, R., Groner, B., and Friis, R.R. (1989). New mammary epithelial and fibroblastic cell clones in coculture form structures competent to differentiate functionally. J. Cell Biol. *108*, 1127–1138.

Reichmann, E., Schwarz, H., Deiner, E.M., Leitner, I., Eilers, M., Berger, J., Busslinger, M., and Beug, H. (1992). Activation of an inducible c-FosER fusion protein causes loss of epithelial polarity and triggers epithelial-fibroblastoid cell conversion. Cell *71*, 1103–1116.

Richards, A.H., and Hilf, R. (1972). Influence of pregnancy, lactation and involution on glucose-6-phosphate dehydrogenase and lactate dehydrogenase in the rat mammary gland. Endocrinology *91*, 287–295.

Rolfe, D.F., and Brown, G.C. (1997). Cellular energy utilization and molecular origin of standard metabolic rate in mammals. Physiol. Rev. *77*, 731–758.

Sekine, N., Cirulli, V., Regazzi, R., Brown, L.J., Gine, E., Tamarit-Rodriguez, J., Girotti, M., Marie, S., MacDonald, M.J., Wollheim, C.B., et al. (1994). Low lactate dehydrogenase and high mitochondrial glycerol phosphate dehydrogenase in pancreatic β-cells. Potential role in nutrient sensing. J. Biol. Chem. *269*, 4895–4902.

Semenza, G.L., Artemov, D., Bedi, A., Bhujwalla, Z., Chiles, K., Feldser, D., Laughner, E., Ravi, R., Simons, J., Taghavi, P., and Zhong, H. (2001). 'The metabolism of tumours': 70 years later. Novartis Found. Symp. *240*, 251–260.

Shim, H., Dolde, C., Lewis, B.C., Wu, C.S., Dang, G., Jungmann, R.A., Dalla-Favera, R., and Dang, C.V. (1997). c-Myc transactivation of LDH-A: implications for tumor metabolism and growth. Proc. Natl. Acad. Sci. USA *94*, 6658–6663.

Stockwell, B.R., Haggarty, S.J., and Schreiber, S.L. (1999). High-throughput screening of small molecules in miniaturized mammalian cell-based assays involving post-translational modifications. Chem. Biol. *6*, 71–83.

Warburg, O. (1930). The Metabolism of Tumors (London: Arnold Constable).

Zarbl, H., Latreille, J., and Jolicoeur, P. (1987). Revertants of v-fos-transformed fibroblasts have mutations in cellular genes essential for transformation by other oncogenes. Cell *51*, 357–369.